

# Phenomenology of texture one zero Yukawa matrix in a flavor symmetric scotogenic model

Lavina Sarma<sup>1,\*</sup> and Mrinal Kumar Das<sup>1,†</sup>

<sup>1</sup>*Department of Physics, Tezpur University, Tezpur 784028, India*

## Abstract

The scotogenic model is well known for accomodating small neutrino mass and dark matter. We have here realised the scotogenic model with the help of discrete flavor symmetry  $A_4 \otimes Z_4$ . We have obtained three one zero textures of Yukawa coupling matrices from the model and have studied its impact on neutrino phenomenology and related aspects of cosmology. On the basis of  $\mu - \tau$  symmetry, we have further discarded two structures of one zero texture Yukawa coupling matrix. We further analyse if the effective mass of active neutrinos obtained by the virtue of the Yukawa coupling matrix is consistent with the KamLAND-Zen limit for  $0\nu\beta\beta$ . Also different lepton flavor violating(LFV) proceses such as  $l_\alpha \rightarrow l_\beta\gamma$  and  $l_\alpha \rightarrow 3l_\beta$  are implemented and their influence on neutrino phenomenology is studied corresponding to the Yukawa coupling matrix. The entire work is carried out considering the dark matter mass( $M_{DM}$ ) in the region 450 – 750 GeV. We have also obtained some significant results for baryon asymmetry of the Universe in agreement with the one zero textures of the coupling matrices. Furthermore, interesting results for relic abundance on the basis of distinct mass splittings between the inert scalars.

---

\* lavina@tezu.ernet.in

† mkdas@tezu.ernet.in

## I. INTRODUCTION

We are familiar with the immense accomplishment of the Standard Model(SM) in explaining the theory for fundamental particles and its interactions. In spite of being an affluent and self-consistent model, it is certainly incomplete. Various observations point towards the need for physics beyond the Standard Model(BSM). This includes the non-zero mass of neutrinos[1], Baryon Asymmetry of the Universe(BAU)[2–9], Dark Matter(DM)[10, 11], etc. The neutrino oscillations[12, 13] has revealed that the neutrinos are massive[14] and also the fact that their flavors mix. The recent Neutrino experiments MINOS[15],RENO[16],T2K[17],Double-Chooz[18] have not only confirmed but also measured the neutrino oscillation parameters more accurately. Also there are significant lines of evidence of DM which comprises of observations in galaxy cluster by Fritz Zwicky [19] in 1933, gravitational lensing (which could allow galaxy cluster to act as gravitational lenses as postulated by Zwicky in 1937) [20], galaxy rotation curves in 1970 [21], cosmic microwave background [22] and the most recent cosmology data given by Planck satellite [23]. From the recent Planck satellite data, it is certain that approximately 27% of the present Universe is comprised of DM, which is about five times more than the baryonic matter. Together with the cosmic baryon asymmetry of the Universe, we have explicit reasons to extend the SM with new particles and fields. We are well aware of the various beyond the Standard model frameworks which tends to incorporate the explanations for the above mentioned anomalies. This includes the seesaw mechanisms such as type I[5], type II[24], type III[25], inverse[26, 27] and radiative seesaws[28–30].

In our work, we mainly focus on the radiative seesaw mechanism which is of much significance in connecting neutrino and dark matter phenomenology. We consider the scotogenic model[31–33] which is an extension of the SM by three heavy neutral singlet fermions and an inert scalar doublet. These extra fields in the extension are experimentally observable at the forthcoming Large Hadron Collider(LHC), with an important implication that the lightest of them could be a significant candidate for the dark matter of the Universe. We basically realise the generic scotogenic model with the help of discrete flavor symmetry  $A_4 \otimes Z_4$ [34]. With proper choice of vacuum expectation value(vev), allowed by  $A_4$  symmetry[35], we are able to generate three structures of Yukawa coupling matrices with one zero texture. We further investigate the phenomenology related with these matrices in both neutrino as well as cosmology sector. A comparative study between the three cases is carried out, thereby determining which one could be viable in satisfying the bounds

from various observations. Neutrinoless double beta decay process[36, 37] is evaluated to check if the effective mass of the active neutrinos abide by the limit given by KamLAND-Zen[38, 39]. Consecutively, we have studied the lepton flavor violating(LFV) proceses such as  $l_\alpha \rightarrow l_\beta \gamma$  and  $l_\alpha \rightarrow 3l_\beta$ , to examine their impression on the neutrino phenomenology. The most stringent bounds on LFV comes from the MEG experiment[40] giving limit on  $\text{Br}(\mu \rightarrow e\gamma) < 4.2 \times 10^{-13}$ . In case of  $l_\alpha \rightarrow 3l_\beta$  decay, bound from SINDRUM experiment[41] is set to be  $\text{BR}(l_\alpha \rightarrow 3l_\beta) < 10^{-12}$ . We have analysed  $N_1$  leptogenesis[2, 3, 34] in all the three cases of Yukawa coupling matrices as it is has a direct consequence in the generation of baryon asymmetry of the Universe. The mass of the lightest heavy neutral singlet fermion is of TeV scale, which has a lower limit  $M_1 \simeq 10$  TeV[3, 42]. Thus, a low scale leptogenesis, generally termed as vanilla leptogenesis is also possible in a scotogenic model unlike other seesaw mechanisms. Our work is primarily carried out with the dark matter candidate(in our case, lightest of the inert scalar doublet) having mass in the regime  $450 - 750$  GeV. However, as seen in various literatures[29, 43, 44], in the IHDM desert, i.e.,  $M_W < M_{DM} \leq 550$  GeV, the generation of relic abundance is prohibited. But, with proper choice of the mass splitting between the scalars and fine tuning of the quartic coupling, it is possible to get the observed relic abundance for  $400 \leq M_{DM} \leq 550$  GeV.

We know that the Yukawa coupling in scotogenic model responsible for generating neutrino mass and freeze-out of dark matter, also significantly persuade lepton flavor violating processes such as  $l_\alpha \rightarrow l_\beta \gamma$  and  $\mu \rightarrow e$  conversion at one loop level. In order to naturally suppress these decays, we can consider the choice of parameters, mainly the elements of Yukawa coupling matrix to play a vital role. One such possibility is obtained by assigning two zeroes simultaneously in the Yukawa coupling matrices. However, this choice leads to a disfavoured range of the UPMNS mixing angles according to the  $3\sigma$  global fit data[45]. Therefore, we take the assumption of one zero texture in Yukawa coupling matrix to obtain a suppressed lepton flavor violating processes simultaneously obeying the  $3\sigma$  range for neutrino oscillation parameters. Furthermore, we proceed the entire phenomenological study taking into consideration of the one zero texture Yukawa coupling matrix which is more preferable as also studied in[45, 46]. In various neutrino mass models as studied in the literatures[47, 48], the allowance of two zero texture on basis of neutrino oscillation parameters is obtained. It is seen to abide by the KamLAND-Zen limit for effective neutrino mass as well. Also as mentioned in[47], where the phenomenological study of texture zeroes in (2,3) inversesee

seesaw is carried out, we see that the higher texture zero structures are disallowed, whereas all the possible structures of texture two zero is successful in producing the desired results for  $0\nu\beta\beta$  and relic abundance of dark matter candidate.

We have further categorised the paper into seven sections which are as follows. Sec.(II) and sec.(III) includes the generic scotogenic model and the flavor symmetric scotogenic model respectively. Phenomenologies such as lepton flavor violation, leptogenesis, and dark matter are mentioned in sec.(IV), sec.(V) and sec.(VI) respectively. We finally show the results and numerical analysis of our work in sec.(VII), finally followed by the conclusion in sec.(VIII).

## II. SCOTOGENIC MODEL

Scotogenic model is an extension of the inert Higgs doublet model (IHDM)[43, 49–52] which is a minimal extension of the SM by a scalar doublet( $\eta$ ). However, IHDM could only accommodate dark matter, but failed to explain the origin of neutrino masses at a renormalizable level. Thus, a modification was required which was made by adding three neutral singlet fermions  $N_i$  with  $i = 1, 2, 3$ . Under a built-in discrete  $Z_2$  symmetry [29, 49, 53–55],  $N_i$  and  $\eta$  are odd whereas the SM fields remain  $Z_2$  even. Symbolic transformation of the particles under  $Z_2$  symmetry is given by,

$$N_i \longrightarrow -N_i, \quad \eta \longrightarrow -\eta, \quad \phi \longrightarrow \phi, \quad \Psi \longrightarrow \Psi, \quad (2.1)$$

where  $\eta$  is the inert Higgs doublet,  $\phi$  is the SM Higgs doublet and  $\Psi$  denotes the SM fermions. The new leptonic and scalar particle content can thereafter be represented as follows under the group of symmetries  $SU(2) \times U(1)_Y \times Z_2$ :

$$\begin{aligned} \begin{pmatrix} \nu_\alpha \\ l_\alpha \end{pmatrix}_L &\sim (2, -\frac{1}{2}, +), \quad l_\alpha^c \sim (1, 1, +), \quad \begin{pmatrix} \phi^+ \\ \phi^0 \end{pmatrix} \sim (2, \frac{1}{2}, +), \\ N_i &\sim (1, 1, -), \quad \begin{pmatrix} \eta^+ \\ \eta^0 \end{pmatrix} \sim (2, 1/2, -). \end{aligned} \quad (2.2)$$

The scalar doublets are written as follows :

$$\eta = \begin{pmatrix} \eta^\pm \\ \frac{1}{\sqrt{2}}(\eta_R^0 + i\eta_I^0) \end{pmatrix}, \quad \phi = \begin{pmatrix} \phi^+ \\ \frac{1}{\sqrt{2}}(h + i\xi) \end{pmatrix}. \quad (2.3)$$

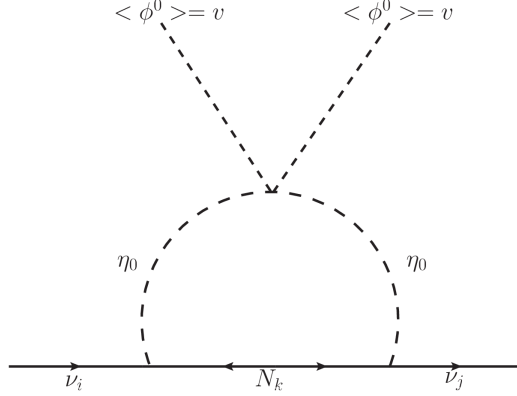


FIG. 1: One- loop contribution of neutrino mass generation with the exchange of right handed neutrino  $N_i$  and the scalar  $\eta_0$ .

We have no Dirac mass term with  $\nu$  and  $N_i$ , however, the similar Yukawa-like coupling involving  $\eta$  is allowed. Nevertheless, the scalar cannot get a VEV. The neutrino mass can be generated through a one-loop mechanism, which is based on the exchange of  $\eta$  particle and a heavy neutrino. In figure, we see two Higgs fields  $\phi^0$  are involved. They will not propagate but will acquire VEV after the EWSB. The lagrangian involving the newly added field is :

$$\mathcal{L} \supset \frac{1}{2}(M_N)_{ij}N_iN_j + Y_{ij}\bar{L}\tilde{\eta}N_j + h.c \quad (2.4)$$

where, the 1<sup>st</sup> term is the Majorana mass term for the neutrino singlet and the 2<sup>nd</sup> term is the Yukawa interactions of the lepton. The new potential on addition of the new inert scalar doublet is:

$$V_{Scalar} = m_1^2\phi^+\phi + m_2^2\eta^+\eta + \frac{1}{2}\lambda_1(\phi^+\phi)^2 + \frac{1}{2}\lambda_2(\eta^+\eta)^2 + \lambda_3(\phi^+\phi)(\eta^+\eta) + \lambda_4(\phi^+\eta)(\eta^+\phi) + \frac{1}{2}\lambda_5[(\phi^+\eta)^2 + h.c.] \quad (2.5)$$

All the parameters in Eq. (2.5) are real by hermicity of the Lagrangian, except for  $\lambda_5$ . Since, the bilinear term  $(\phi^+\eta)$  is forbidden by the exact  $Z_2$  symmetry, therefore one can always choose  $\lambda_5$

real by rotating the relative phase between  $\phi$  and  $\eta$ . Furthermore, after the spontaneous symmetry breaking like in the SM, we are left with one physical Higgs boson  $h$  which resembles the SM Higgs boson, as well as four dark scalars: one CP even( $\eta_R^0$ ), one CP odd( $\eta_I^0$ ) and a pair of charged ones ( $\eta^\pm$ ). The masses of these physical scalars are:

$$\begin{aligned}
m_h^2 &= -m_1^2 = 2\lambda_1 v^2, \\
m_{\eta^\pm}^2 &= m_2^2 + \lambda_3 v^2, \\
m_{\eta_R^0}^2 &= m_2^2 + (\lambda_3 + \lambda_4 + \lambda_5) v^2, \\
m_{\eta_I^0}^2 &= m_2^2 + (\lambda_3 + \lambda_4 - \lambda_5) v^2.
\end{aligned}
\tag{2.6}$$

It is clear from the above equations that all the scalar couplings are written in terms of physical scalar masses and  $m_2$ , thereby providing six independent parameters of the model to be :  $\{m_2, m_h, m_{\eta_R^0}, m_{\eta_I^0}, m_{\eta^\pm}, \lambda_2\}$ . Here,  $m_h$  is the mass of SM-Higgs,  $m_{\eta_R^0}$ ,  $m_{\eta_I^0}$  and  $m_{\eta^\pm}$  are the masses of CP-even, CP-odd and charged scalars of the inert doublet respectively. In this work, as we have considered the CP-even scalar to be the lightest particle and a probable DM candidate, so we consider  $\lambda_5 < 0$  without any loss of generality. Also, the limit  $\lambda_5 \rightarrow 0$  leads to the mass degeneracy of the neutral components of the inert doublet. Following the 't Hooft scenario[56], the smallness of  $\lambda_5$  to obtain the lepton asymmetry, which would have been lost if considered to be zero, is acceptably natural. We have a simplified diagram shown in Fig.(2) that can be split further into two diagrams and from which the mass can be easily calculated by considering mechanism after EWSB.

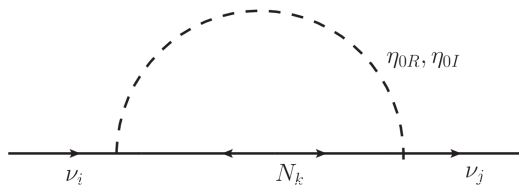


FIG. 2: One-loop diagram with exchange of  $\eta_R^0$  and  $\eta_I^0$ .  $\nu_i$  and  $\nu_j$  representing two different generations of active neutrinos.  $N_i$  is the right handed neutrino.

Calculation on the basis of one diagram is sufficient and considered as other would be same except for  $\eta_R^0$  replaced by  $\eta_I^0$ . The neutrino mass matrix arising from the radiative mass model is

Field	$l$	$e_R$	$\mu_R$	$\tau_R$	$H$	$\eta$	$\chi$	$\chi'$	$\chi''$	$\phi$	$\kappa$	$\kappa'$	$N_1$	$N_2$	$N_3$
$A_4$	3	1	1''	1'	1	1	3	3	3	3	1	1'	1	1'	1
$Z_4$	1	$i$	$i$	$i$	1	1	1	$i$	-1	- $i$	1	-1	1	- $i$	-1

TABLE I: Fields and their respective transformations under the symmetry group of the model.

given by :

$$\begin{aligned}
M_{ij}^\nu &= \sum_k \frac{Y_{ik} Y_{jk}}{16\pi^2} M_k \left[ \frac{m_{\eta_R}^2}{m_{\eta_R}^2 - M_k^2} \ln \frac{m_{\eta_R}^2}{M_k^2} - \frac{m_{\eta_I}^2}{m_{\eta_I}^2 - M_k^2} \ln \frac{m_{\eta_I}^2}{M_k^2} \right] \\
&\equiv \sum_k \frac{Y_{ik} Y_{jk}}{16\pi^2} M_k [L_k(m_{\eta_R}^2) - L_k(m_{\eta_I}^2)],
\end{aligned} \tag{2.7}$$

where  $M_k$  represents the mass eigenvalue of the mass eigenstate  $N_k$  of the neutral singlet fermion  $N_k$  in the internal line with indices  $j=1,2,3$  running over the three neutrino generation with three copies of  $N_k$  and  $Y$  is the Yukawa coupling matrix. The function  $L_k(m^2)$  used in Eq. (2.7) is given by:

$$L_k(m^2) = \frac{m^2}{m^2 - M_k^2} \ln \frac{m^2}{M_k^2} \tag{2.8}$$

### III. $A_4 \otimes Z_4$ SYMMETRIC SCOTOGENIC MODEL

With the help of discrete flavor symmetry, in our case  $A_4 \otimes Z_4$ , we realise the minimal scotogenic model and obtain the neutrino mass at 1-loop level with the DM candidate contained. The discrete symmetries, i.e  $A_4 \times Z_4$  will impose constraints on the Yukawa coupling matrix, thereby, constraining the model. In our work, we obtain three cases of texture one zero Yukawa coupling matrix by the virtue of the choice of the vev. Furthermore, using these distinct Yukawa coupling matrices, we determine the neutrino mass and analyse the phenomenologies associated with it. The particle content and their respective charges corresponding to the discrete symmetries are given in Table I. We have the  $A_4 \otimes Z_4$  invariant Lagrangian for the lepton sector as follows:

$$\begin{aligned}
\mathcal{L} \supset & \frac{y_e}{\Lambda} (\bar{l} H \phi) e_R + \frac{y_\mu}{\Lambda} (\bar{l} H \phi) \mu_R + \frac{y_\tau}{\Lambda} (\bar{l} H \phi) \tau_R + \frac{y_1}{\Lambda} (\bar{l} \eta \chi) N_1 + \frac{y_2}{\Lambda} (\bar{l} \eta \chi') N_2 + \frac{y_3}{\Lambda} (\bar{l} \eta \chi'') N_3 + \\
& \frac{1}{2} \omega_1 \kappa \bar{N}_1^c N_1 + \frac{1}{2} \omega_2 \kappa' \bar{N}_2^c N_2 + \frac{1}{2} \omega_3 \kappa \bar{N}_3^c N_3
\end{aligned} \tag{3.1}$$

Terms in the first parenthesis represents the product of two triplets( $l$  and  $\phi$ ) under  $A_4$ , where each of these terms contracts with  $A_4$  singlets  $1, 1'$  and  $1''$  corresponding to  $e_R, \mu_R$  and  $\tau_R$  respectively. With the choice of vacuum expectation value of the flavon  $\phi$ , i.e.  $\langle \phi \rangle = (v, 0, 0)$ , we obtain the flavor structure for charged lepton coupling matrix to be a diagonal one. The charged lepton mass matrix is given by:

$$M_l = \frac{\langle H \rangle v}{\Lambda} \begin{bmatrix} y_e & 0 & 0 \\ 0 & y_\mu & 0 \\ 0 & 0 & y_\tau \end{bmatrix} \quad (3.2)$$

Because of the additional  $Z_4$  symmetry, the right handed neutrino mass matrix will be diagonal one with  $\langle \kappa \rangle = \langle \kappa' \rangle = v$ .

$$M_R = \begin{bmatrix} \omega_1 v & 0 & 0 \\ 0 & \omega_2 v & 0 \\ 0 & 0 & \omega_3 v \end{bmatrix}, \quad (3.3)$$

where  $\omega_1, \omega_2$  and  $\omega_3$  are the Majorana couplings. As we have mentioned earlier that we tend to obtain three texture one zero Yukawa coupling matrices from this model. This is possible depending on the choice of vev assigned to the flavons  $\chi, \chi'$  and  $\chi''$ .

Case I: Incorporating the following flavon allignments:  $\langle \chi \rangle = (0, -v, v)$ ,  $\langle \chi' \rangle = (v, v, v)$  and  $\langle \chi'' \rangle = (v, v, v)$  in Eq.(3.1), we obtain a zero term in  $Y'_{11}$  position given by:

$$Y' = \begin{bmatrix} 0 & b & c \\ -a & b & c \\ a & b & c \end{bmatrix}, \quad (3.4)$$

where  $a = y_1 \frac{v}{\Lambda}$ ,  $b = y_2 \frac{v}{\Lambda}$  and  $c = y_3 \frac{v}{\Lambda}$ .

Case II: We obtain a zero in the  $Y''_{13}$  position of the Yukawa coupling matrix from Eq.(3.1) with a slight alteration in the assignment of vev allignment of the flavons as such:  $\langle \chi \rangle = (v, v, v)$ ,  $\langle \chi' \rangle = (v, v, v)$  and  $\langle \chi'' \rangle = (0, -v, v)$ . The Yukawa coupling matrix takes the form:

$$Y'' = \begin{bmatrix} a & b & 0 \\ a & b & -c \\ a & b & c \end{bmatrix}. \quad (3.5)$$

Case III: Again with the choice of vev allignments given by:  $\langle \chi \rangle = (v, v, v)$ ,  $\langle \chi' \rangle = (0, -v, v)$

and  $\langle \chi'' \rangle = (v, v, v)$ , the term in the  $Y_{22}'''$  position turns out to be zero. Thus, the Yukawa coupling matrix in this case is expressed as:

$$Y''' = \begin{bmatrix} a & b & c \\ a & 0 & c \\ a & -b & c \end{bmatrix}. \quad (3.6)$$

Considering these three cases for the Yukawa coupling matrices, we carry out our analysis in various sector. Incorporating the three cases of Yukawa coupling matrix in Eq.2.7, we obtain a  $\mu - \tau$  symmetry for Case I and Case II. A broken  $\mu - \tau$  symmetry is obtained naturally only in Case III. Thus, we study the phenomenology for Case III, as it is the only viable structure of one zero texture Yukawa coupling matrix in our model.

#### IV. LEPTON FLAVOR VIOLATION

No experiment so far has observed a flavor violating process involving charged leptons. However, many experiments are currently going on to set strong limits on the most relevant LFV observables, in order to constraint parameter space involved in many new physics models. In this section we will discuss various lepton flavor violating processes (LFV) such as  $l_\alpha \rightarrow l_\beta \gamma, l_\alpha \rightarrow 3l_\beta$  and  $\mu - e$  conversion in nuclei[57, 58]. Currently muon decay experiments are most prominent in nature which provides stringent limits for most models. The MEG collaboration[40] has been able to set the impressive bound on muon decay  $\text{BR}(l_\alpha \rightarrow l_\beta \gamma) < 4.2 \times 10^{-13}$ . This is expected to improve as the experiment is upgraded to MEG II. In case of  $l_\alpha \rightarrow 3l_\beta$  decay, constraints comes from SINDRUM experiment[41] to be  $\text{BR}(l_\alpha \rightarrow 3l_\beta) < 10^{-12}$  which is set long ago. The future Mu3e experiment announces a sensitivity of  $10^{-16}$ , which would imply a 4 orders of magnitude improvement on the current bound.

The neutrinoless  $\mu - e$  conversion of muonic atom is the most interesting developments regarding the LFV processes[59]. There are many experiments which will basically aim for the positive signal. DeeMe[60], Mu2e[61], COMET[62] and PRIME[63] are such experiments primarily focusing on  $\mu - e$  conversion of muonic atom. The sensitivity of these experiments will range from  $10^{-14}$  to  $10^{-18}$ . The current limits on  $\tau$  observables are less stringent, but will also get improved in the near future by the LHC collaboration, as well as by B-factories such as Belle II[64]. In this part we will discuss

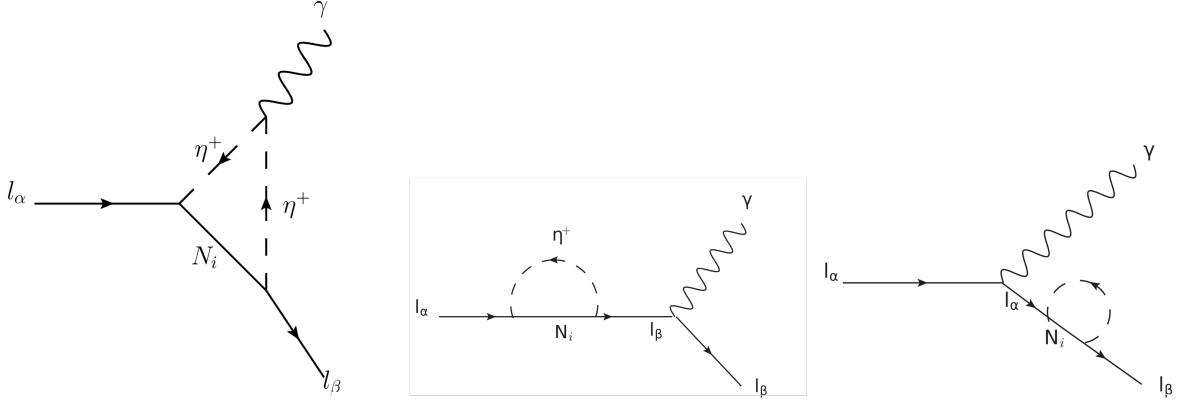


FIG. 3: The 1-loop Feynman diagrams giving rise to  $l_\alpha \rightarrow l_\beta \gamma$ .

the analytical results of branching ratios of different LFV processes such as  $l_\alpha \rightarrow l_\beta \gamma$ ,  $l_\alpha \rightarrow 3l_\beta$  and  $\mu - e$  conversion in nuclei within the framework of scotogenic model.

In case of radiative lepton decay, the branching ratio of  $l_\alpha \rightarrow l_\beta \gamma$  is given by[65]-

$$\text{BR}(l_\alpha \rightarrow l_\beta \gamma) = \frac{3(4\pi^3)\alpha_{\text{em}}}{4G_F^2} |A_D|^2 \text{BR}(l_\alpha \rightarrow l_\beta \nu_\alpha \bar{\nu}_\beta). \quad (4.1)$$

Here,  $G_F$  is the Fermi constant and  $\alpha_{\text{em}} = \frac{e^2}{4\pi}$  is the electromagnetic fine structure constant, with  $e$  the electromagnetic coupling.  $A_D$  is the dipole form factor which is given by-

$$A_D = \sum_{i=1}^3 \frac{Y_{i\beta}^* Y_{i\alpha}}{2(4\pi)^2 m_{\eta^+}^2} F_2(\rho_i) \quad (4.2)$$

where the parameter  $\rho_i$  is defined as  $\rho_i = \frac{M_i^2}{m_{\eta^+}^2}$  and the loop function  $F_2(x)$  is given in appendix.

For three body decay process like  $l_\alpha \rightarrow 3l_\beta$ , the branching ratio is given by-

$$\begin{aligned} \text{BR}(l_\alpha \rightarrow 3l_\beta) = & \frac{3(4\pi^2)\alpha_{\text{em}}^2}{8G_F^2} \left[ |A_{\text{ND}}|^2 + |A_D|^2 \left( \frac{16}{3} \log \left( \frac{m_\alpha}{m_\beta} \right) - \frac{22}{3} \right) \right. \\ & \left. + \frac{1}{6} |B|^2 + \left( -2A_{\text{ND}} A_D^* + \frac{1}{3} A_{\text{ND}} B^* - \frac{2}{3} A_D B^* + \text{h.c.} \right) \right] \\ & \times \text{BR}(l_\alpha \rightarrow l_\beta \nu_\alpha \bar{\nu}_\beta). \end{aligned} \quad (4.3)$$

Here, we have kept  $m_\beta \ll m_\alpha$  only in the logarithmic term, where it avoids the appearance of an infrared divergence. The form factor  $A_D$  is generated by dipole photon penguins and is given in equation 17. Regarding the other form factors  $A_{\text{ND}}$  is given by-

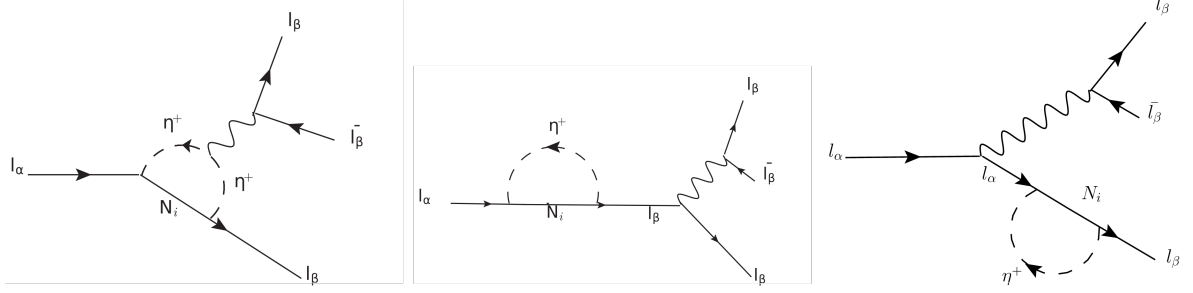


FIG. 4: The penguin contributions to  $l_\alpha \rightarrow l_\beta \gamma$ , where the wavy lines depicts either a Z-boson or a photon.

$$A_{ND} = \sum_{i=1}^3 \frac{Y_{i\beta}^* Y_{i\alpha}}{6(4\pi)^2 m_{\eta^+}^2} G_2(\rho_i). \quad (4.4)$$

$A_{ND}$  is generated by non-dipole photon penguins, whereas B, induced by box diagrams is given by-

$$e^2 B = \frac{1}{(4\pi)^2 m_{\eta^+}^2} \sum_{i,j=1}^3 \left[ \frac{1}{2} D_1(\rho_i, \rho_j) Y_{j\beta}^* Y_{j\beta} Y_{i\beta}^* Y_{i\alpha} + \sqrt{\rho_i \rho_j} D_2(\rho_i, \rho_j) Y_{j\beta}^* Y_{j\beta}^* Y_{i\beta} Y_{i\alpha} \right]. \quad (4.5)$$

The loop functions  $G_2(x)$ ,  $D_1(x, y)$  and  $D_2(x, y)$  are defined in appendix. Here, e Z-boson penguin contributions are negligible, since in this model they are suppressed by charged lepton masses. Similarly, Higgs-penguin contribution is also suppressed which are not taken into consideration. Next we consider the case of  $\mu - e$  conversion in nuclei. The conversion rate, normalized to the muon capture rate, can be expressed as -

$$\text{CR}(\mu - e, \text{Nucleus}) = \frac{p_e E_e m_\mu^3 G_F^2 \alpha_{\text{em}}^3 Z_{\text{eff}}^4 F_p^2}{8\pi^2 Z \Gamma_{\text{capt}}} \times \left[ |(Z + N)(g_{LV}^{(0)} + g_{LS}^{(0)}) + (Z - N)(g_{LV}^{(1)} + g_{LS}^{(1)})|^2 + |(Z + N)(g_{RV}^{(0)} + g_{RS}^{(0)}) + (Z - N)(g_{RV}^{(1)} + g_{RS}^{(1)})|^2 \right] \quad (4.6)$$

here, number of photon and neutron is given by Z and N.  $Z_{\text{eff}}$  is the effective atomic charge,  $F_p$  denotes the nuclear matrix element and total muon capture rate is denoted by  $\Gamma_{\text{capt}}$ . The values of these parameter are different for different nucleus under consideration. Also,  $p_e$  and  $E_e$  are the momentum and energy of electron. The expression for  $g_{XK}^{(0)}$  and  $g_{XK}^{(1)}$  ( $X=L, R$  and  $K=S, V$ ) present in the above equation is given by-

$$g_{XK}^{(0)} = \frac{1}{2} \sum_{q=u,d,s} \left( g_{XK}(q) G_K^{q,p} + g_{XK}(q) G_K^{q,n} \right) \quad (4.7)$$

$$g_{XK}^{(1)} = \frac{1}{2} \sum_{q=u,d,s} \left( g_{XK}(q) G_K^{q,p} - g_{XK}(q) G_K^{q,n} \right). \quad (4.8)$$

Numerical values of  $G_K$  are given in various literatures. Again the effective couplings  $g_{XK}(q)$  in scotogenic model has many contributions, which are given below-

$$g_{LV}(q) \approx g_{LV}^\gamma(q) \quad (4.9)$$

$$g_{RV}(q) = g_{LV}(q)|_{L \leftrightarrow R} \quad (4.10)$$

$$g_{LS}(q) \approx 0 \quad (4.11)$$

$$g_{RS}(q) \approx 0 \quad (4.12)$$

where  $g_{LV}^\gamma(q)$  stands for the contribution due to photon penguins. Because of the inbuilt  $Z_2$  symmetry in scotogenic model, there is no box contribution to  $\mu - e$  conversion of nuclei. This additional symmetry forbids the coupling between scalars( $\eta^+$  and  $\eta^-$ ) and the quark sector. Regarding the Z-boson penguins contributions, they turn out to be suppressed by charged lepton masses. So the effective coupling can be written as-

$$g_{LV}^\gamma(q) = \frac{\sqrt{2}}{G_F} e^2 Q_p (A_{ND} - A_D). \quad (4.13)$$

The form factors  $A_{ND}$  and  $A_D$  have been already defined. Furthermore,  $Q_p$  is the electric charge of the corresponding quark.

## V. BARYON ASYMMETRY OF THE UNIVERSE

We study baryogenesis in the Scotogenic model realised by  $A_4 \times Z_4$  symmetry. We can produce observed baryogenesis via the mechanism of leptogenesis[2] in our model. However, the leptogenesis process must occur by the out of equilibrium decay of the RHN, in our case  $N_1$ . As discussed in many literatures[66, 67], we now know that there exists a lower bound of about 10TeV for the lightest of the RHNs( $M_1$ ) in the Scotogenic model considering the vanilla leptogenesis scenario[3, 33]. For a heirarchical mass of RHN, i.e  $M_1 \ll M_2, M_3$ , the leptogenesis produced by the decay of  $N_2$  and  $N_3$  are suppressed due to the strong washout effects produced by  $N_1$  or  $N_2$  and  $N_3$  mediated interactions[33]. Thereby, the lepton asymmetry is produced only by the virtue of  $N_1$

decay and this is further converted into the baryon asymmetry of the Universe(BAU) by the electro-weak sphaleron phase transitions[68]. Now for the generation of BAU, we solve the simultaneous Boltzmann equations for  $N_1$  decay and formation of  $N_{B-L}$ . The B-L calculation depends on the comparison between the decay rates for  $N_1 \rightarrow l\eta, \bar{l}\eta^*$  processes and the Hubble parameter, which causes a certain impact on the asymmetry as well as on the CP-asymmetry parameter  $\epsilon_1$ . In the calculation of leptogenesis, one important quantity that differentiates between weak and strong washout regime is the decay parameter. It is expressed as:

$$K_1 = \frac{\Gamma_1}{H(z=1)}, \quad (5.1)$$

where,  $\Gamma_2$  gives us the total  $N_2$  decay width,  $H$  is the Hubble parameter and  $z = \frac{M_1}{T}$  with  $T$  being the temperature of the photon bath. We can express  $H$  in terms of  $T$  and the corresponding equation is given by:

$$H = \sqrt{\frac{8\pi^3 g_*}{90}} \frac{T^2}{M_{Pl}}. \quad (5.2)$$

In Eq.(5.2),  $g_*$  stands for the effective number of relativistic degrees of freedom and  $M_{Pl} \simeq 1.22 \times 10^{19}$  GeV is the Planck mass. We consider the RHN masses as  $M_1 = 10^4 - 10^5$  GeV,  $M_2 = 10^6 - 10^7$  GeV and  $M_3 = 5 \times 10^7 - 10^8$  GeV. Now, by this choice of RHN masses along with  $m_{\eta_R^0} = 450 - 750$  GeV and most significantly the lightest active neutrino mass  $m_l = 10^{-13} - 10^{-11}$  eV, we fall on the weak washout regime. The Yukawa couplings obtained by solving the model parameters are incorporated in the decay rate equation for  $N_1$  which is given by,

$$\Gamma_1 = \frac{M_1}{8\pi} (Y^\dagger Y)_{11} \left[ 1 - \left( \frac{m_{\eta_R^0}}{M_1} \right)^2 \right]^2 = \frac{M_1}{8\pi} (Y^\dagger Y)_{11} (1 - \eta_1)^2 \quad (5.3)$$

Again for the decays  $N_1 \rightarrow l\eta, \bar{l}\eta^*$ , the CP asymmetry parameter  $\epsilon_1$  is given by,

$$\epsilon_1 = \frac{1}{8\pi (Y^\dagger Y)_{11}} \sum_{j \neq 1} \text{Im}[(Y^\dagger Y)^2]_{1j} \left[ f(r_{j1}, \eta_1) - \frac{\sqrt{r_{j1}}}{r_{j1} - 1} (1 - \eta_1)^2 \right], \quad (5.4)$$

where,

$$f(r_{j1}, \eta_1) = \sqrt{r_{j1}} \left[ 1 + \frac{(1 - 2\eta_1 + r_{j1})}{(1 - \eta_1)^2} \ln \left( \frac{r_{j1} - \eta_1^2}{1 - 2\eta_1 + r_{j1}} \right) \right], \quad (5.5)$$

and  $r_{j1} = \left( \frac{M_j}{M_1} \right)^2$ ,  $\eta_1 \equiv \left( \frac{m_{\eta_R^0}}{M_1} \right)^2$ .

The Boltzmann equations for the number densities of  $N_1$  and  $N_{B-L}$ , given by [66],

$$\frac{dn_{N_1}}{dz} = -D_1 (n_{N_1} - n_{N_1}^{eq}), \quad (5.6)$$

$$\frac{dn_{B-L}}{dz} = -\epsilon_1 D_1 (n_{N_1} - n_{N_1}^{eq}) - W_1 n_{B-L}, \quad (5.7)$$

respectively.  $n_{N_1}^{eq} = \frac{z^2}{2} K_1(z)$  is the equilibrium number density of  $N_1$ , where  $K_i(z)$  is the modified Bessel function of  $i^{th}$  type and

$$D_1 \equiv \frac{\Gamma_1}{Hz} = K_{N_1} z \frac{K_1(z)}{K_2(z)} \quad (5.8)$$

gives the measure of the total decay rate with respect to the Hubble rate, and  $W_1 = \frac{\Gamma_W}{Hz}$  is the total washout rate. Again,  $W_1 = W_{1D} + W_{\Delta L=2}$ , i.e the total washout term is the sum of the washout due to inverse decays  $l\eta, \bar{l}\eta^* \rightarrow N_1$  ( $W_{1D} = \frac{1}{4} K_{N_1} z^3 K_1(z)$ ) and the washout due to the  $\Delta L = 2$  scatterings  $l\eta \leftrightarrow \bar{l}\eta^*, ll \leftrightarrow \eta^*\eta^*$  which is given by,

$$W_{\Delta L=2} \simeq \frac{18\sqrt{10}M_{Pl}}{\pi^4 g_l \sqrt{g_*} z^2 v^4} \left(\frac{2\pi^2}{\lambda_5}\right)^2 M_1 \bar{m}_\zeta^2. \quad (5.9)$$

Here,  $g_l$  is the internal degrees of freedom for the SM leptons, and  $\bar{m}_\zeta$  is the effective neutrino mass parameter, defined by:

$$\bar{m}_\zeta^2 \simeq 4\varsigma_1^2 m_1^2 + \varsigma_2 m^2 + \varsigma_3^2 m_3^2, \quad (5.10)$$

where  $m'_i$ 's are the light neutrino mass eigenvalues and  $\varsigma_k$  is defined as:

$$\varsigma_k = \left( \frac{M_k^2}{8(m_{\eta_R}^2 - m_{\eta_I}^2)} [L_k(m_{\eta_R}^2) - L_k(m_{\eta_I}^2)] \right)^{-1} \quad (5.11)$$

The final B-L asymmetry  $n_{B-L}^f$  is evaluated by numerically calculating Eq.(5.6) and Eq.(5.7) before the sphaleron freeze-out. This is converted into the baryon-to-photon ratio given by:

$$n_B = \frac{3}{4} \frac{g_*^0}{g_*} a_{sph} n_{B-L}^f \simeq 9.2 \times 10^{-3} n_{B-L}^f, \quad (5.12)$$

In Eq.(5.12),  $g_* = 110.75$  is the effective relativistic degrees of freedom at the time when final lepton asymmetry was produced,  $g_*^0 = \frac{43}{11}$  is the effective degrees of freedom at the recombination epoch and  $a_{sph} = \frac{8}{23}$  is the sphaleron conversion factor taking two Higgs doublet into consideration. The Planck limit 2018 gives a bound on the observed BAU( $n_B^{obs}$ ) to be  $(6.04 \pm 0.08) \times 10^{-10}$ [69]. Therefore, in our work we have chosen the free parameters appropriately so as to generate the observed BAU. The values of the quartic coupling,  $\lambda_5$  is taken in range  $10^{-3} - 1$  for successful generation of leptogenesis as well as to have significant results for LFV.

## VI. SCALAR DARK MATTER

The dark matter loses its equilibrium state when the pair annihilation rate becomes less than the expansion rate of the Universe, eventually leading the particles to decouple from the cosmic plasma. The relic densities of such thermally produced dark matter candidates can be calculated by solving the Boltzmann equation [70, 71]:

$$\dot{n}_{DM} + 3Hn_{DM} = - \langle \sigma v \rangle (n_{DM}^2 - (n_{DM}^{eq})^2), \quad (6.1)$$

where,  $n_{DM}$  is the number density of the dark matter candidate and  $n_{DM}^{eq}$  is the number density of the dark matter candidate in thermal equilibrium. The numerical solution of the Boltzmann equation in terms of partial wave expansion,  $\langle \sigma v \rangle = a + bv^2$  is of the form,

$$\Omega h^2 \approx \frac{1.04 \times 10^9 x_f}{M_{Pl} \sqrt{g_*} (a + 3b/x_f)}, \quad (6.2)$$

where,  $x_f = \frac{m_{DM}}{T_f}$ ,  $T_f$  is the freeze-out temperature, also  $v^2 \simeq \frac{6}{x_f}$ ,  $m_{DM}$  is the mass of dark matter,  $g_*$  is the number of relativistic degrees of freedom at the time of freeze-out, and  $M_{Pl} \approx 1.22 \times 10^{19}$  GeV is the Planck mass. Furthermore, we can also express this above expression in a simpler analytical form for the approximation of DM relic abundance as [72],

$$\Omega h^2 \approx \frac{3 \times 10^{-27} \text{cm}^3 \text{s}^{-1}}{\langle \sigma v \rangle} \quad (6.3)$$

The corresponding thermal averaged annihilation cross section is therefore given by[73];

$$\langle \sigma v \rangle = \frac{1}{8m_{DM}^4 T K_2^2(m_{DM}/T)} \int_{4m_{DM}^2}^{\infty} \sigma(s - 4m_{DM}^2) \sqrt{s} K_1(\sqrt{s}/T) ds, \quad (6.4)$$

where,  $K_1$  and  $K_2$  are the modified Bessel functions,  $m_{DM}$  is the mass of dark matter candidate and  $T$  is the temperature. In this  $A_4$  realisation of the scotogenic model, the lightest of the neutral component of the scalar doublet  $\eta$ , i.e.  $\eta^0$  is considered to be the dark matter candidate. [43, 44, 49, 51, 53–55, 74–81]. From the literature [82], we can express the effective cross-section as,

$$\sigma_{eff} = \sum_{i,j}^N \langle \sigma_{ij} v \rangle \frac{g_i g_j}{g_{eff}^2} (1 + \Delta_i)^{3/2} (1 + \Delta_j)^{3/2} e^{(-x_f(\Delta_i + \Delta_j))}, \quad (6.5)$$

with,  $\Delta_i = \frac{m_i - m_{DM}}{m_{DM}}$  and  $g_{eff} = \sum_{i=1}^N g_i (1 + \Delta_i)^{3/2} e^{-x_f \Delta_i}$ .

In the above equation,  $m_i$  denotes the mass of the heavier inert Higgs doublet. Therefore, the expression for the thermally averaged cross section is given by

$$\langle \sigma_{ij} v \rangle = \frac{x_f}{8m_i^2 m_j^2 m_{DM} K_2\left(\frac{m_i x_f}{m_{DM}}\right) K_2\left(\frac{m_j x_f}{m_{DM}}\right)} \times \int_{(m_i+m_j)^2}^{\infty} \sigma_{ij}(s-2(m_i^2+m_j^2)) \sqrt{s} K_1\left(\frac{\sqrt{s} x_f}{m_{DM}}\right) ds. \quad (6.6)$$

In our work, we have shown the relic abundance for a certain range of dark matter, i.e  $M_{DM} = 450 - 750$  GeV by the usage of a computational package `MicrOmega 5.0.4`[83]. Due to the choice of RHN masses being heavier than the DM mass, its influence in the dark matter sector is negligible, i.e. it doesn't alter the relic abundance generated for the lightest inert scalar.

The only parameters mainly affecting the relic is the DM-Higgs coupling ( $\lambda_L$ ) and the mass differences between the inert scalars. By appropriate choice of  $\lambda_L$  and mass splitting, it is possible to generate the correct relic abundance for DM mass around 450-500 GeV. We have done a comparative study so as to show how crucial the mass splitting between the inert scalar can be for the production of observed relic abundance. We have chosen two cases,  $\Delta M_{\eta^\pm} = \Delta M_{\eta_I^0} = 8$  GeV and  $\Delta M_{\eta^\pm} = \Delta M_{\eta_I^0} = 0.9$  GeV respectively in Fig.6, where we can observe that for small mass splitting the relic is achieved for  $M_{DM} \sim 480$  GeV, whereas for large mass splitting we get the relic for DM mass above 500 GeV. From Fig.5, we have analysed the parameter space of  $\lambda_L$  for two different values of scalar mass splittings which satisfy the Planck limit for relic abundance of DM. The left panel of Fig.5 corresponds to  $\Delta M_{\eta^\pm} = \Delta M_{\eta_I^0} = 8$  GeV, where the DM mass satisfying the observed relic abundance limit is above 580 GeV for the values of  $\lambda_L$  upto  $0.08 \times 10^{-2}$ . Whereas for  $\Delta M_{\eta^\pm} = \Delta M_{\eta_I^0} = 0.9$  GeV, relic abundance is satisfied for  $M_{DM} \sim 490 - 500$  GeV for the same range of  $\lambda_L$  as can be seen in the right panel of Fig.5.

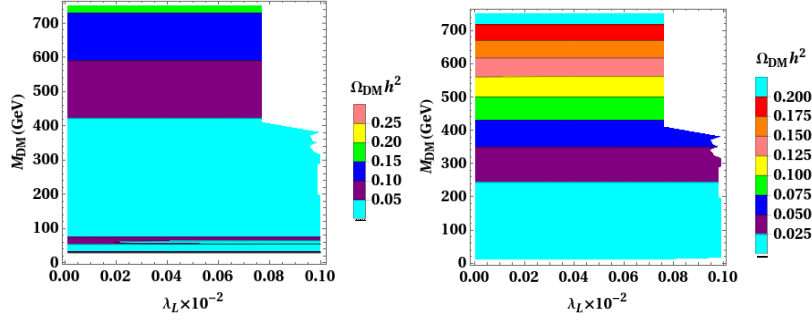


FIG. 5: Contour plot between the DM-Higgs coupling  $\lambda_L$  and DM mass  $M_{DM}$  w.r.t the allowed space of relic abundance of DM. The left panel is for  $\Delta M_{\eta^\pm} = \Delta M_{\eta_I^0} = 8$  GeV and the right panel is for  $\Delta M_{\eta^\pm} = \Delta M_{\eta_I^0} = 0.9$  GeV

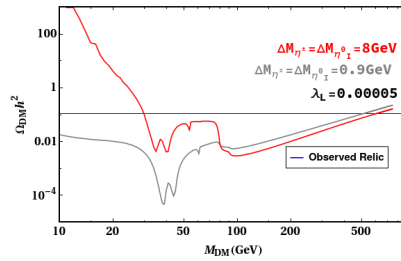


FIG. 6: Variational plot between relic abundance of DM ( $\Omega_{DM}h^2$ ) and DM mass( $M_{DM}$ ) with benchmark value  $\lambda_L = 0.00005$  for two different values of mass splitting between inert scalars, i.e.  $\Delta M_{\eta^\pm} = \Delta M_{\eta_I^0} = 8$  GeV and  $\Delta M_{\eta^\pm} = \Delta M_{\eta_I^0} = 0.9$  GeV.

## VII. RESULTS AND ANALYSIS

We have discussed in Sec.III an  $A_4 \otimes Z_4$  extension of the minimal Scotogenic model. By the choice of three different sets of vev alignment, we are able to show three distinct structures of Yukawa coupling matrices bearing a zero component in one of the matrix elements. However, two of the structures can be discarded from the  $\mu - \tau$  symmetry point of view. The first two cases of one zero texture are seen to take the form of  $\mu - \tau$  symmetry when incorporated in the mass matrix of the model. We are therefore left with only one structure of one zero texture Yukawa coupling matrix which breaks the  $\mu - \tau$  symmetry and thus is allowed in the model. Analysing the

neutrino phenomenology of this matrix structure in our work, we therefore, calculate the effective mass of the active neutrinos( $m_{\beta\beta}$ ). The experimental technique of detecting neutrino mass i.e. neutrinoless double beta decay( $0\nu\beta\beta$ )[36, 37, 84] includes some well known experiments related to it such as KamLAND-Zen[38, 39], GERDA[85, 86], KATRIN[87, 88]. The expression for  $m_{\beta\beta}$  is given by:

$$|m_{\beta\beta}| = \sum_{k=1}^3 m_k U_{ek}^2 \quad (7.1)$$

where,  $U_{ek}^2$  are the elements of the neutrino mixing matrix with  $k$  holding up the generation index. This eq.(7.1) can be further expressed as,

$$|m_{\beta\beta}| = |m_1 U_{ee}^2 + m_2 U_{e\nu}^2 + m_3 U_{e\tau}^2|. \quad (7.2)$$

Also, a special yet one of the most popular types of parametrization known as the *Casas-Ibarra parametrization* [89] is used in our work to numerical obtain the solutions of the model parameters. This parametrization is used in order to link the Yukawa coupling with the light neutrino parameters.

$$Y = U \sqrt{M_\nu^{diag}} R^\dagger \sqrt{\Lambda}, \quad (7.3)$$

where  $R$  is a complex orthogonal matrix satisfying the condition  $R^T R = 1$ . As per our convenience, the orthogonal complex matrix  $R$  takes the form,

$$R = \begin{pmatrix} 0 & 0 & 1 \\ \cos Z & -\sin Z & 0 \\ \sin Z & \cos Z & 0 \end{pmatrix}, \quad (7.4)$$

which can be further expressed as:

$$R = \begin{pmatrix} 0 & 0 & 1 \\ \theta & -\sqrt{1-\theta^2} & 0 \\ \sqrt{1-\theta^2} & \theta & 0 \end{pmatrix}, \quad (7.5)$$

where,  $\theta = \cos Z$ . The numerical value of  $\theta$  is solved for the three different structures of the Yukawa coupling matrix.

Since Case I and Case II are discarded, we carry out our study only considering Case III.

### A. Case III:

Again on interchanging the choice of vev alignment of the flavons  $\chi$ ,  $\chi'$  and  $\chi''$ , we can achieve a Yukawa coupling matrix with one zero element at the  $Y_{22}'''$  position as given in Eq.3.6. As analysed earlier in the previous subsections, we follow a similar study for this particular structure of  $Y'''$ . From Fig.7, we see that in the plot for NH, all the points fall on the allowed region as per the KamLAND-Zen limit. However, in the right panel of Fig.7, i.e. for IH,  $m_l = 10^{-19} - 10^{-16}$  eV is successful in generating the effective mass of active neutrinos in the allowed region. We show variation of different parameters vs baryon asymmetry of the Universe in Fig.8. For NH, the mass range considered for  $M_1$  satisfies the BAU limit given by Planck, however we have maximum points only in the region  $M_1 = 4 \times 10^4 - 10^5$  GeV in case of IH which generates the desired BAU. The parameter space of  $\lambda_5$  satisfying the BAU constraint is between  $10^{-1} - 1$  for both NH and IH. In the third row of Fig.8, we can conclude a definite range of lightest active neutrino which produces the desired BAU. For NH,  $m_l = 10^{-19} - 10^{-17}$  eV and for IH,  $m_l = 10^{-18} - 10^{-16}$  eV obeys the Planck limit for BAU. Again, considering the variation of  $M_{DM}$  as a function of BAU, the entire range of DM mass, i.e.  $M_{DM} = 450 - 750$  GeV is seen to satisfy the Planck limit for BAU in case of both NH as well as IH. Unlike the other cases discussed above, here the orthogonal matrix R for NH has no variation in the matrix elements, i.e. the absolute value of all elements is found to be 1. Therefore, in Fig.9, contour plots of only a,b and c w.r.t  $m_{\beta\beta}$  is shown. However, we obtain a different matrix for IH, thus we have shown plots considering its variation with other model parameters w.r.t  $m_{\beta\beta}$  as can be seen in Fig.10. The allowed parameter space for the model parameters considered from the Fig9 and Fig.10 is shown in a tabular form in Tab.II. In case III, we can draw analysis from Fig.11 and Fig.12 that the variations of  $\rho_N$  and  $m_l$  w.r.t the branching ratios and conversion ratio is same for both NH and IH. Thus, we have  $Br(\mu \rightarrow 3e)$  lies in the range  $10^{-49} - 10^{-39}$  and  $Br(\mu \rightarrow e\gamma) \sim 10^{-26} - 10^{-22}$  w.r.t  $\rho_N$  and  $m_l$ . And the conversion ratio ranges from  $Cr(\mu \rightarrow e, Ti) \sim 10^{-49} - 10^{-39}$ . In our attempt to co-relate the BAU and the effective mass of neutrinos  $m_{\beta\beta}$ , we have shown a co-relation plot in Fig.13. Here, we observe that for  $m_{\beta\beta} = 10^{-4} - 10^{-3}$ eV the desired BAU is obtained in NH, whereas for IH,  $m_{\beta\beta} = 10^{-2} - 10^{-1}$ eV is the allowed range generating correct BAU.

Parameter	NH	IH
a	$0.05 \times 10^{-8} - 0.2 \times 10^{-8}$	$0.02 \times 10^{-10} - 0.10 \times 10^{-10}$
b	$0.01 \times 10^{-7} - 0.15 \times 10^{-7}$	$0.03 \times 10^{-3} - 0.35 \times 10^{-3}$
c	$0.1 \times 10^{-3} - 0.7 \times 10^{-3}$	$0.1 \times 10^{-3} - 1.6 \times 10^{-3}$
$\theta$	1	0.7 - 1.9

TABLE II: Model parameters of the model and their respective parameter space satisfying effective mass of light neutrinos( $m_{\beta\beta}$ ) for Case III.

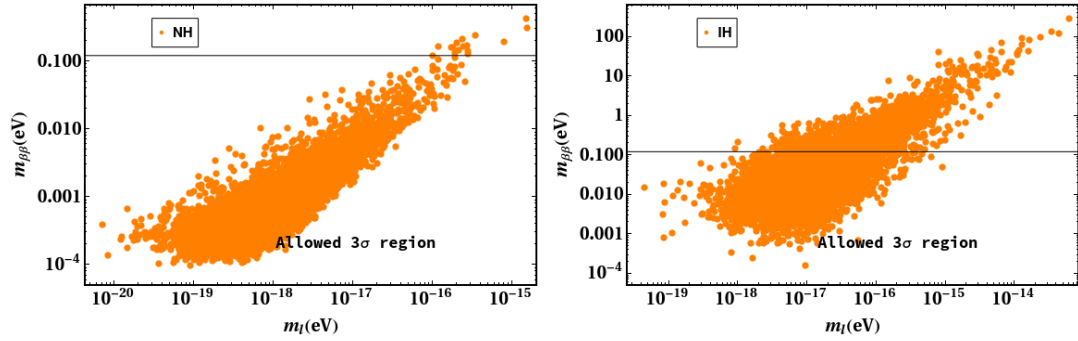


FIG. 7: Lightest active neutrino mass( $m_l$ ) as a function of effective mass( $m_{\beta\beta}$ ) for NH/IH for Case III. The horizontal(black) line depicts the upper bound on the effective mass ( $m_{\beta\beta}(eV) \sim 0.1(eV)$ ) of light neutrinos obtained from KamLAND-Zen experiment.

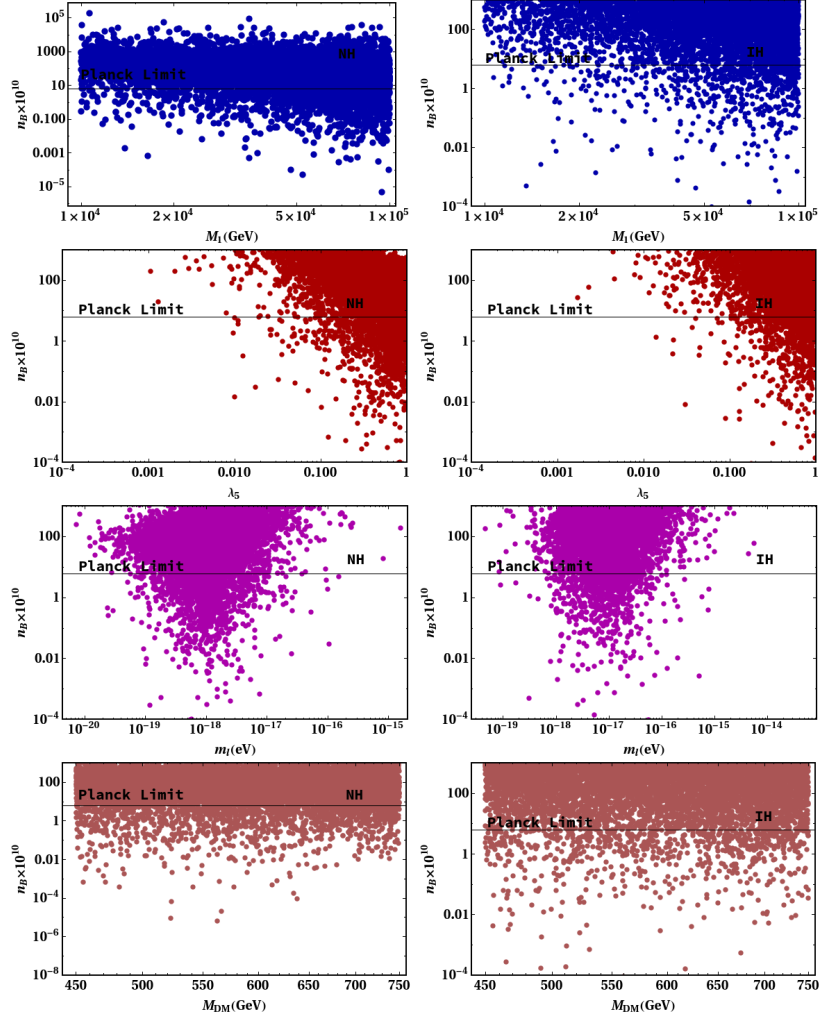


FIG. 8: Plots in the first-row shows baryon asymmetry as a function of RHN ( $M_1$ ), the second-row shows baryon asymmetry as a function of the quartic coupling ( $\lambda_5$ ), in third-row baryon asymmetry as a function of lightest neutrino mass eigenvalue( $m_l$ ) is depicted and in the fourth row we show a plot between dark matter mass( $M_{DM}$ ) and BAU respectively for Case III. The black horizontal line gives the current Planck limit for BAU.

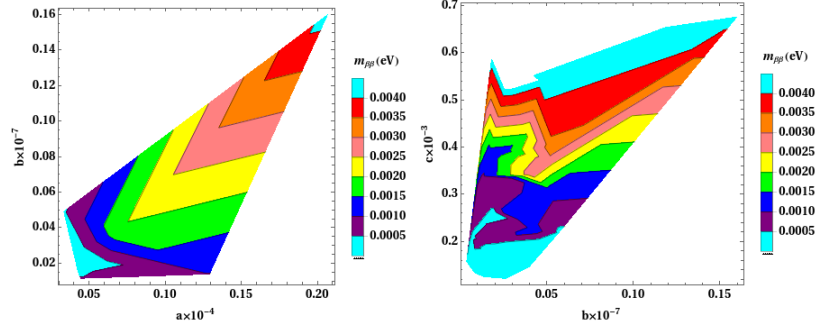


FIG. 9: Contour plot showing the parameter space of model parameters a,b and c w.r.t effective mass( $m_{\beta\beta}$ ) for NH for Case III.

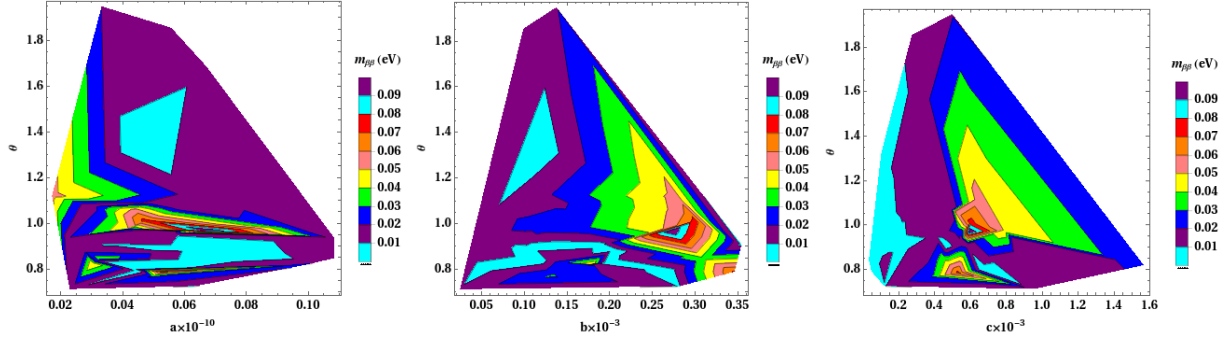


FIG. 10: Contour plot showing the parameter space of model parameters a,b,c and rotational angle  $\theta$  w.r.t effective mass( $m_{\beta\beta}$ ) for IH for Case III.

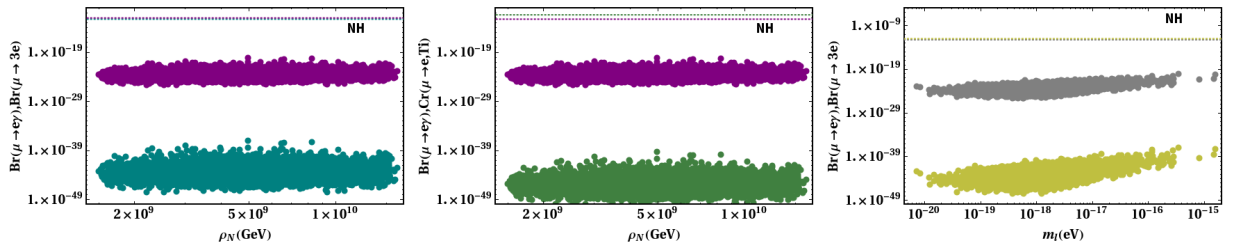


FIG. 11: Plot on the left panel shows  $Br(\mu \rightarrow e\gamma)$  and  $Br(\mu \rightarrow 3e)$  as a function of  $\rho_N$  (where  $\rho_N = (\frac{M_N}{m_{\eta^+}})^2$ ), plot in the middle depicts  $Br(\mu \rightarrow e\gamma)$  and  $Cr(\mu \rightarrow e, Ti)$  as a function of  $\rho_N$  and the right panel shows a variation between  $Br(\mu \rightarrow e\gamma)$  and  $Br(\mu \rightarrow 3e)$  w.r.t the lightest neutrino mass eigenvalue( $m_1$ ) for NH of Case III. The dashed horizontal lines are the recent upper bounds.

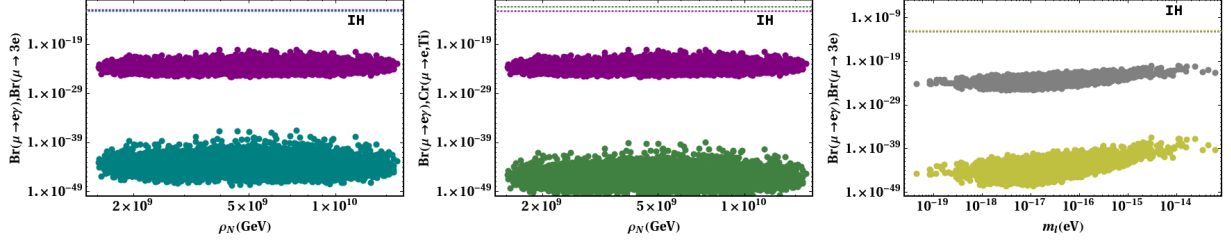


FIG. 12: Plot on the left panel shows  $Br(\mu \rightarrow e\gamma)$  and  $Br(\mu \rightarrow 3e)$  as a function of  $\rho_N$  (where  $\rho_N = (\frac{M_N}{m_{\eta^+}})^2$ ), plot in the middle depicts  $Br(\mu \rightarrow e\gamma)$  and  $Cr(\mu \rightarrow e, Ti)$  as a function of  $\rho_N$  and the right panel shows a variation between  $Br(\mu \rightarrow e\gamma)$  and  $Br(\mu \rightarrow 3e)$  w.r.t the lightest neutrino mass eigenvalue( $m_l$ ) for IH of Case III. The dashed horizontal lines are the recent upper bounds.

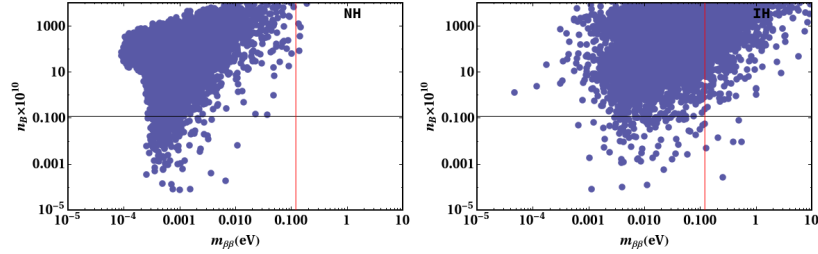


FIG. 13: A variation between the effective mass of active neutrinos( $m_{\beta\beta}$ ) and baryon asymmetry of the Universe( $n_B$ ) is shown for Case III. The black horizontal line gives the Planck bound on BAU and the red vertical line is the upper limit on the effective mass ( $m_{\beta\beta}(eV) \sim 0.1(eV)$ ) of light neutrinos obtained from KamLAND-Zen experiment.

Analogous to the framework based on texture zeroes studied in [48], where it is seen that the results obtained for LFV are not very satisfactory incase of two zero texture compared to that in one zero texture. Also as already mentioned in [45], two zero texture has been discarded from the LFV point of view. Thus, we have solely generated only one zero texture of the Yukawa coupling matrix from our model to study its significance in neutrino sector.

## VIII. CONCLUSION

We have extensively studied the scotogenic model realised with the help of discrete flavor symmetries  $A_4 \otimes Z_4$ . Our work mainly focuses on the condition required to generate texture one zero in the Yukawa coupling matrix. The various vev alignments mandatory in this aspect is been discussed in Sec.III. With due change in the consideration of the vev alignments of the flavons  $\chi$ ,  $\chi'$  and  $\chi''$ , we are able to construct three different structures of Yukawa coupling matrix with a zero element in it. Since, broken  $\mu - \tau$  symmetry is a crucial requirement, two structures of Yukawa coupling matrix (i.e. Case I and Case II) are forbidden and only Case III is allowed. Additionally, we take some particular range of free parameters such as  $M_1 = 10^4 - 10^5$  GeV,  $M_2 = 10^6 - 10^7$  GeV,  $M_3 = 5 \times 10^7 - 10^8$  GeV,  $m_{\eta_R^0} = 450 - 750$  GeV,  $m_l = 10^{-13} - 10^{-11}$  eV and  $\lambda_5 = 10^{-3} - 1$ , and proceed with the calculation of various phenomena for the allowed Yukawa coupling matrix. In order to make the model feasible, we have studied the neutrino phenomenology like  $0\nu\beta\beta$ , lepton flavor violation and also have added a pinch of cosmology via BAU. The one zero texture matrix in eq.3.6 is evaluated in our work. We see that the allowed Case III satisfies the KamLAND-Zen limit and Planck limit for  $m_{\beta\beta}$  and BAU respectively from Fig.7 and Fig.8. Thus, from the extensive analysis we have carried out, we can consider Case III to abide by the experimental constraints alongwith a naturally broken  $\mu - \tau$  symmetry. Furthermore, for the validity of the model w.r.t dark matter phenomenology, we have assumed the dark matter(lightest of the inert doublet scalar) mass  $M_{DM}$  in the range 450-750 GeV. As we have considered two distinct values of the mass splittings between the inert scalars, we can draw conclusion that for the lower value of mass splitting, i.e.  $\Delta M_{\eta^\pm} = \Delta M_{\eta_l^0} = 0.9$  GeV, a wider range of allowed DM mass is obtained. The consistency of this result is shown for a benchmark value of DM-Higgs coupling  $\lambda_L = 0.00005$  as well as for quite a broad space of  $\lambda_L$  as can be seen in Fig.5 and Fig.6. Thus, as a whole we can contemplate this discrete flavor realisation of the scotogenic model to be sound in explaining various beyond standard model phenomenologies and also plays a crucial role in distinguishing between the most

desirable structure of the Yukawa coupling matrices.

---

- [1] P. de Salas, D. Forero, C. Ternes, M. Tortola, and J. Valle, “Status of neutrino oscillations 2018:  $3\sigma$  hint for normal mass ordering and improved CP sensitivity,” *Phys. Lett. B* **782** (2018) 633–640, [arXiv:1708.01186 \[hep-ph\]](#).
- [2] M. Fukugita and T. , “Baryogenesis Without Grand Unification,” *Phys. Lett. B* **174** (1986) 45–47.
- [3] T. Hogle, M. Platscher, and K. Schmitz, “Low-Scale Leptogenesis in the Scotogenic Neutrino Mass Model,” *Phys. Rev. D* **98** no. 2, (2018) 023020, [arXiv:1804.09660 \[hep-ph\]](#).
- [4] **Particle Data Group** Collaboration, M. Tanabashi *et al.*, “Review of Particle Physics,” *Phys. Rev. D* **98** no. 3, (2018) 030001.
- [5] P. Minkowski, “ $\mu \rightarrow e\gamma$  at a Rate of One Out of  $10^9$  Muon Decays?,” *Phys. Lett. B* **67** (1977) 421–428.
- [6] R. N. Mohapatra and G. Senjanovic, “Neutrino Mass and Spontaneous Parity Nonconservation,” *Phys. Rev. Lett.* **44** (1980) 912.
- [7] T. Yanagida, “Horizontal gauge symmetry and masses of neutrinos,” *Conf. Proc. C* **7902131** (1979) 95–99.
- [8] J. Schechter and J. Valle, “Neutrino Masses in SU(2) x U(1) Theories,” *Phys. Rev. D* **22** (1980) 2227.
- [9] S. Glashow, “The Future of Elementary Particle Physics,” *NATO Sci. Ser. B* **61** (1980) 687.
- [10] G. Bertone, D. Hooper, and J. Silk, “Particle dark matter: Evidence, candidates and constraints,” *Phys. Rept.* **405** (2005) 279–390, [arXiv:hep-ph/0404175](#).
- [11] B. Moore, S. Ghigna, F. Governato, G. Lake, T. R. Quinn, J. Stadel, and P. Tozzi, “Dark matter substructure within galactic halos,” *Astrophys. J. Lett.* **524** (1999) L19–L22, [arXiv:astro-ph/9907411](#).
- [12] **Super-Kamiokande** Collaboration, Y. Fukuda *et al.*, “Evidence for oscillation of atmospheric neutrinos,” *Phys. Rev. Lett.* **81** (1998) 1562–1567, [arXiv:hep-ex/9807003](#).
- [13] **SNO** Collaboration, Q. R. Ahmad *et al.*, “Direct evidence for neutrino flavor transformation from neutral current interactions in the Sudbury Neutrino Observatory,” *Phys. Rev. Lett.* **89** (2002)

- 011301, [arXiv:nucl-ex/0204008](https://arxiv.org/abs/nucl-ex/0204008).
- [14] **Planck** Collaboration, M. Lattanzi, “Planck 2015 constraints on neutrino physics,” *J. Phys. Conf. Ser.* **718** no. 3, (2016) 032008.
- [15] **MINOS** Collaboration, P. Adamson *et al.*, “Improved search for muon-neutrino to electron-neutrino oscillations in MINOS,” *Phys. Rev. Lett.* **107** (2011) 181802, [arXiv:1108.0015](https://arxiv.org/abs/1108.0015) [hep-ex].
- [16] **RENO** Collaboration, J. K. Ahn *et al.*, “Observation of Reactor Electron Antineutrino Disappearance in the RENO Experiment,” *Phys. Rev. Lett.* **108** (2012) 191802, [arXiv:1204.0626](https://arxiv.org/abs/1204.0626) [hep-ex].
- [17] **T2K** Collaboration, K. Abe *et al.*, “Indication of Electron Neutrino Appearance from an Accelerator-produced Off-axis Muon Neutrino Beam,” *Phys. Rev. Lett.* **107** (2011) 041801, [arXiv:1106.2822](https://arxiv.org/abs/1106.2822) [hep-ex].
- [18] **Double Chooz** Collaboration, Y. Abe *et al.*, “Indication of Reactor  $\bar{\nu}_e$  Disappearance in the Double Chooz Experiment,” *Phys. Rev. Lett.* **108** (2012) 131801, [arXiv:1112.6353](https://arxiv.org/abs/1112.6353) [hep-ex].
- [19] F. Zwicky, “Die Rotverschiebung von extragalaktischen Nebeln,” *Helv. Phys. Acta* **6** (1933) 110–127.
- [20] T. Treu, P. Marshall, and D. Clowe, “Resource Letter: Gravitational Lensing,” *Am. J. Phys.* **80** (2012) 753, [arXiv:1206.0791](https://arxiv.org/abs/1206.0791) [astro-ph.CO].
- [21] V. C. Rubin and J. Ford, W.Kent, “Rotation of the Andromeda Nebula from a Spectroscopic Survey of Emission Regions,” *Astrophys. J.* **159** (1970) 379–403.
- [22] R. Durrer, “The cosmic microwave background: the history of its experimental investigation and its significance for cosmology,” *Class. Quant. Grav.* **32** no. 12, (2015) 124007, [arXiv:1506.01907](https://arxiv.org/abs/1506.01907) [astro-ph.CO].
- [23] **Planck** Collaboration, P. Ade *et al.*, “Planck 2015 results. XXIV. Cosmology from Sunyaev-Zeldovich cluster counts,” *Astron. Astrophys.* **594** (2016) A24, [arXiv:1502.01597](https://arxiv.org/abs/1502.01597) [astro-ph.CO].
- [24] S. Antusch and S. King, “Type ii leptogenesis and the neutrino mass scale,” *Phys. Lett., B* **597** no. 2, (2004) 199 – 207.  
<http://www.sciencedirect.com/science/article/pii/S0370269304010317>.

- [25] R. Foot, H. Lew, X. G. He, and G. C. Joshi, “See-saw neutrino masses induced by a triplet of leptons,” *Zeitschrift für Physik C Particles and Fields* **44** no. 3, (Sep, 1989) 441–444.  
<https://doi.org/10.1007/BF01415558>.
- [26] M. Hirsch, S. Morisi, and J. Valle, “A4-based tri-bimaximal mixing within inverse and linear seesaw schemes,” *Phys. Lett., B* **679** no. 5, (2009) 454 – 459.  
<http://www.sciencedirect.com/science/article/pii/S0370269309009174>.
- [27] S. Khalil, “TeV-scale gauged b- l symmetry with inverse seesaw mechanism,” *Phys. Rev., D* **82** no. 7, (2010) 077702.
- [28] E. Ma, “Pathways to naturally small neutrino masses,” *Phys. Rev. Lett.* **81** (1998) 1171–1174, [arXiv:hep-ph/9805219](https://arxiv.org/abs/hep-ph/9805219).
- [29] E. Ma, “Verifiable radiative seesaw mechanism of neutrino mass and dark matter,” *Phys. Rev. D* **73** (2006) 077301, [arXiv:hep-ph/0601225](https://arxiv.org/abs/hep-ph/0601225).
- [30] E. Ma and U. Sarkar, “Radiative Left-Right Dirac Neutrino Mass,” *Phys. Lett. B* **776** (2018) 54–57, [arXiv:1707.07698](https://arxiv.org/abs/1707.07698) [hep-ph].
- [31] E. Ma, “Verifiable radiative seesaw mechanism of neutrino mass and dark matter,” *Phys. Rev. D* **73** (2006) 077301, [arXiv:hep-ph/0601225](https://arxiv.org/abs/hep-ph/0601225).
- [32] L. Sarma, P. Das, and M. K. Das, “Scalar dark matter and leptogenesis in the minimal scotogenic model,” [arXiv:2004.13762](https://arxiv.org/abs/2004.13762) [hep-ph].
- [33] D. Borah, P. B. Dev, and A. Kumar, “TeV scale leptogenesis, inflaton dark matter and neutrino mass in a scotogenic model,” *Phys. Rev. D* **99** no. 5, (2019) 055012, [arXiv:1810.03645](https://arxiv.org/abs/1810.03645) [hep-ph].
- [34] B. B. Boruah, L. Sarma, and M. K. Das, “Lepton flavor violation and leptogenesis in discrete flavor symmetric scotogenic model,” [arXiv:2103.05295](https://arxiv.org/abs/2103.05295) [hep-ph].
- [35] H. Zhang, “Light Sterile Neutrino in the Minimal Extended Seesaw,” *Phys. Lett. B* **714** (2012) 262–266, [arXiv:1110.6838](https://arxiv.org/abs/1110.6838) [hep-ph].
- [36] R. Mohapatra, “New Contributions to Neutrinoless Double beta Decay in Supersymmetric Theories,” *Phys. Rev. D* **34** (1986) 3457–3461.
- [37] J. Barry and W. Rodejohann, “Lepton number and flavour violation in TeV-scale left-right symmetric theories with large left-right mixing,” *JHEP* **09** (2013) 153, [arXiv:1303.6324](https://arxiv.org/abs/1303.6324) [hep-ph].

- [38] **KamLAND-Zen** Collaboration, Y. Gando, “Neutrinoless double beta decay search with liquid scintillator experiments,” in *Prospects in Neutrino Physics*. 4, 2019. [arXiv:1904.06655](#) [physics.ins-det].
- [39] **KamLAND-Zen** Collaboration, A. Li, “A Bayesian Approach to Neutrinoless Double Beta Decay Analysis in KamLAND-Zen,” *J. Phys. Conf. Ser.* **1468** no. 1, (2020) 012201.
- [40] **MEG** Collaboration, A. Baldini *et al.*, “Search for the lepton flavour violating decay  $\mu^+ \rightarrow e^+\gamma$  with the full dataset of the MEG experiment,” *Eur. Phys. J. C* **76** no. 8, (2016) 434, [arXiv:1605.05081](#) [hep-ex].
- [41] **Mu3e** Collaboration, A.-K. Perrevoort, “Searching for Lepton Flavour Violation with the Mu3e Experiment,” *PoS NuFact2017* (2017) 105, [arXiv:1802.09851](#) [physics.ins-det].
- [42] D. Mahanta and D. Borah, “Fermion dark matter with  $N_2$  leptogenesis in minimal scotogenic model,” *JCAP* **11** (2019) 021, [arXiv:1906.03577](#) [hep-ph].
- [43] L. Lopez Honorez, E. Nezri, J. F. Oliver, and M. H. Tytgat, “The Inert Doublet Model: An Archetype for Dark Matter,” *JCAP* **02** (2007) 028, [arXiv:hep-ph/0612275](#).
- [44] A. Ahriche, A. Jueid, and S. Nasri, “Radiative neutrino mass and Majorana dark matter within an inert Higgs doublet model,” *Phys. Rev. D* **97** no. 9, (2018) 095012, [arXiv:1710.03824](#) [hep-ph].
- [45] A. Ibarra, C. E. Yaguna, and O. Zapata, “Direct Detection of Fermion Dark Matter in the Radiative Seesaw Model,” *Phys. Rev. D* **93** no. 3, (2016) 035012, [arXiv:1601.01163](#) [hep-ph].
- [46] T. Kitabayashi, “Scotogenic dark matter and single-zero textures of the neutrino mass matrix,” *Phys. Rev. D* **98** no. 8, (2018) 083011, [arXiv:1808.01060](#) [hep-ph].
- [47] N. Gautam and M. K. Das, “Impact of texture zeros on dark matter and neutrinoless double beta decay in inverse seesaw,” *Nucl. Phys. B* **971** (2021) 115519, [arXiv:2104.13071](#) [hep-ph].
- [48] H. Borgohain and M. K. Das, “Phenomenology of two texture zero neutrino mass in left-right symmetric model with  $Z_8 \times Z_2$ ,” *JHEP* **02** (2019) 129, [arXiv:1810.04889](#) [hep-ph].
- [49] L. Lopez Honorez and C. E. Yaguna, “The inert doublet model of dark matter revisited,” *JHEP* **09** (2010) 046, [arXiv:1003.3125](#) [hep-ph].
- [50] A. Arhrib, R. Benbrik, and N. Gaur, “ $H \rightarrow \gamma\gamma$  in Inert Higgs Doublet Model,” *Phys. Rev.* **D85** (2012) 095021, [arXiv:1201.2644](#) [hep-ph].

- [51] S. Bhattacharya, P. Ghosh, A. K. Saha, and A. Sil, “Two component dark matter with inert Higgs doublet: neutrino mass, high scale validity and collider searches,” *JHEP* **03** (2020) 090, [arXiv:1905.12583 \[hep-ph\]](#).
- [52] D. Borah, S. Sadhukhan, and S. Sahoo, “Lepton Portal Limit of Inert Higgs Doublet Dark Matter with Radiative Neutrino Mass,” *Phys. Lett. B* **771** (2017) 624–632, [arXiv:1703.08674 \[hep-ph\]](#).
- [53] T. Hambye, F.-S. Ling, L. Lopez Honorez, and J. Rocher, “Scalar Multiplet Dark Matter,” *JHEP* **07** (2009) 090, [arXiv:0903.4010 \[hep-ph\]](#). [Erratum: *JHEP* 05, 066 (2010)].
- [54] E. M. Dolle and S. Su, “The Inert Dark Matter,” *Phys. Rev. D* **80** (2009) 055012, [arXiv:0906.1609 \[hep-ph\]](#).
- [55] M. Gustafsson, S. Rydbeck, L. Lopez-Honorez, and E. Lundstrom, “Status of the Inert Doublet Model and the Role of multileptons at the LHC,” *Phys. Rev. D* **86** (2012) 075019, [arXiv:1206.6316 \[hep-ph\]](#).
- [56] G. ’t Hooft, C. Itzykson, A. Jaffe, H. Lehmann, P. Mitter, I. Singer, and R. Stora, eds., *Recent Developments in Gauge Theories. Proceedings, Nato Advanced Study Institute, Cargese, France, August 26 - September 8, 1979*, vol. 59. 1980.
- [57] A. Ilakovac, “Lepton flavor violation in the standard model extended by heavy singlet Dirac neutrinos,” *Phys. Rev. D* **62** (2000) 036010, [arXiv:hep-ph/9910213](#).
- [58] I. Masina and C. A. Savoy, “Charged Lepton Flavour and CP Violations: Theoretical Impact of Present and Future Experiments,” *Nucl. Phys. B Proc. Suppl.* **143** (2005) 70–75, [arXiv:hep-ph/0410382](#).
- [59] D. Dinh, A. Ibarra, E. Molinaro, and S. Petcov, “The  $\mu - e$  Conversion in Nuclei,  $\mu \rightarrow e\gamma, \mu \rightarrow 3e$  Decays and TeV Scale See-Saw Scenarios of Neutrino Mass Generation,” *JHEP* **08** (2012) 125, [arXiv:1205.4671 \[hep-ph\]](#). [Erratum: *JHEP* 09, 023 (2013)].
- [60] **DeeMe** Collaboration, H. Natori, “An experiment to search for mu-e conversion at J-PARC MLF in Japan, DeeMe experiment,” *PoS ICHEP2018* (2019) 642.
- [61] **Mu2e** Collaboration, S. Miscetti, “Status of the Mu2e experiment at Fermilab,” *EPJ Web Conf.* **234** (2020) 01010.
- [62] **Comet** Collaboration, H. Nishiguchi, “Search for Muon-to-Electron Conversion at J-PARC: COMET Experiment,” *PoS EPS-HEP2017* (2017) 674.

- [63] Y. Kuno, “Lepton flavor violation: Muon to electron conversion, COMET and PRISM/PRIME at J-PARC,” *PoS NUFACT08* (2008) 111.
- [64] **Belle II** Collaboration, T. Konno, “Tau LFV and LNV at Belle II,” *PoS NuFact2019* (2020) 089.
- [65] T. Toma and A. Vicente, “Lepton Flavor Violation in the Scotogenic Model,” *JHEP* **01** (2014) 160, [arXiv:1312.2840 \[hep-ph\]](#).
- [66] S. Davidson and A. Ibarra, “A Lower bound on the right-handed neutrino mass from leptogenesis,” *Phys. Lett. B* **535** (2002) 25–32, [arXiv:hep-ph/0202239](#).
- [67] W. Buchmuller, P. Di Bari, and M. Plumacher, “Cosmic microwave background, matter - antimatter asymmetry and neutrino masses,” *Nucl. Phys. B* **643** (2002) 367–390, [arXiv:hep-ph/0205349](#). [Erratum: *Nucl.Phys.B* 793, 362 (2008)].
- [68] M. Dine and A. Kusenko, “The Origin of the matter - antimatter asymmetry,” *Rev. Mod. Phys.* **76** (2003) 1, [arXiv:hep-ph/0303065](#).
- [69] **Planck** Collaboration, N. Aghanim *et al.*, “Planck 2018 results. VI. Cosmological parameters,” [arXiv:1807.06209 \[astro-ph.CO\]](#).
- [70] R. J. Scherrer and M. S. Turner, “On the Relic, Cosmic Abundance of Stable Weakly Interacting Massive Particles,” *Phys. Rev. D* **33** (1986) 1585. [Erratum: *Phys.Rev.D* 34, 3263 (1986)].
- [71] E. W. Kolb and M. S. Turner, *The Early Universe*, vol. 69. 1990.
- [72] G. Jungman, M. Kamionkowski, and K. Griest, “Supersymmetric dark matter,” *Phys. Rept.* **267** (1996) 195–373, [arXiv:hep-ph/9506380](#).
- [73] P. Gondolo and G. Gelmini, “Cosmic abundances of stable particles: Improved analysis,” *Nucl. Phys. B* **360** (1991) 145–179.
- [74] N. G. Deshpande and E. Ma, “Pattern of Symmetry Breaking with Two Higgs Doublets,” *Phys. Rev. D* **18** (1978) 2574.
- [75] M. Cirelli, N. Fornengo, and A. Strumia, “Minimal dark matter,” *Nucl. Phys. B* **753** (2006) 178–194, [arXiv:hep-ph/0512090](#).
- [76] R. Barbieri, L. J. Hall, and V. S. Rychkov, “Improved naturalness with a heavy Higgs: An Alternative road to LHC physics,” *Phys. Rev. D* **74** (2006) 015007, [arXiv:hep-ph/0603188](#).
- [77] E. Ma, “Suitability of A(4) as a Family Symmetry in Grand Unification,” *Mod. Phys. Lett. A* **21** (2006) 2931–2936, [arXiv:hep-ph/0607190](#).

- [78] D. Borah and A. Gupta, “New viable region of an inert Higgs doublet dark matter model with scotogenic extension,” *Phys. Rev. D* **96** no. 11, (2017) 115012, [arXiv:1706.05034 \[hep-ph\]](#).
- [79] A. Goudelis, B. Herrmann, and O. Stål, “Dark matter in the Inert Doublet Model after the discovery of a Higgs-like boson at the LHC,” *JHEP* **09** (2013) 106, [arXiv:1303.3010 \[hep-ph\]](#).
- [80] A. Arhrib, Y.-L. S. Tsai, Q. Yuan, and T.-C. Yuan, “An Updated Analysis of Inert Higgs Doublet Model in light of the Recent Results from LUX, PLANCK, AMS-02 and LHC,” *JCAP* **06** (2014) 030, [arXiv:1310.0358 \[hep-ph\]](#).
- [81] D. Borah, R. Roshan, and A. Sil, “Minimal two-component scalar doublet dark matter with radiative neutrino mass,” *Phys. Rev. D* **100** no. 5, (2019) 055027, [arXiv:1904.04837 \[hep-ph\]](#).
- [82] K. Griest and D. Seckel, “Three exceptions in the calculation of relic abundances,” *Phys. Rev. D* **43** (1991) 3191–3203.
- [83] G. Bélanger, F. Boudjema, A. Goudelis, A. Pukhov, and B. Zaldivar, “micrOMEGAs5.0 : Freeze-in,” *Comput. Phys. Commun.* **231** (2018) 173–186, [arXiv:1801.03509 \[hep-ph\]](#).
- [84] C. Giunti, “Phenomenology of absolute neutrino masses,” *Nucl. Phys. B Proc. Suppl.* **145** (2005) 231–236, [arXiv:hep-ph/0412148](#).
- [85] **GERDA** Collaboration, M. Agostini *et al.*, “Final Results of GERDA on the Search for Neutrinoless Double- $\beta$  Decay,” *Phys. Rev. Lett.* **125** (2020) 252502, [arXiv:2009.06079 \[nucl-ex\]](#).
- [86] **GERDA** Collaboration, V. D’Andrea, “Neutrinoless double beta decay search with the GERDA experiment,” *Nuovo Cim. C* **43** no. 2-3, (2020) 24.
- [87] **KATRIN** Collaboration, F. Fraenkle, “The neutrino mass experiment KATRIN,” *J. Phys. Conf. Ser.* **1342** no. 1, (2020) 012024.
- [88] **KATRIN** Collaboration, L. Schlüter and T. Lasserre, “First neutrino mass measurement with the KATRIN experiment,” *J. Phys. Conf. Ser.* **1468** no. 1, (2020) 012180.
- [89] J. Casas and A. Ibarra, “Oscillating neutrinos and  $\mu \rightarrow e, \gamma$ ,” *Nucl. Phys. B* **618** (2001) 171–204, [arXiv:hep-ph/0103065](#).